Journal of Porphyrins and Phthalocyanines
J. Porphyrins Phthalocyanines 2010; **14**: 264–270
DOI: 10.1142/S1088424610001969

Published at http://www.worldscinet.com/jpp/

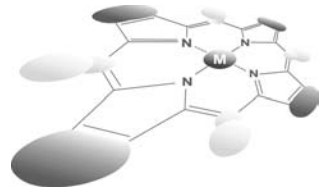

Interaction between novel porphyrin-dextran nanoparticles and human serum albumin

Zhi Zhang[a], Qian-ni Guo[a], Yun-guo Lu[a], Tao Jia[b], Kun Yan*[a] and Zao-ying Li*[a]

[a] *College of Chemistry and Molecular Sciences, Wuhan University, Wuhan 430072, P.R. China*
[b] *College of Pharmacy, Wuhan University, Wuhan 430072, P.R. China*

Received 18 February 2009
Accepted 16 June 2009

ABSTRACT: A novel porphyrin-dextran coated Fe_3O_4 nanoparticle (**5**) was designed and synthesized. The structure of **5** was confirmed by IR, UV-vis and inductively coupled plasma atomic emission spectrometry, and dynamic laser scattering (DLS); magnetic property was measured by a vibrating sample magnetometer (VSM). The interaction between compound **5** and human serum albumin (HSA) was investigated through UV-vis absorbance spectra and fluorospectrophotometer, compared with the 5-(4-aminophenyl)-10,15,20-tris-(4-sulfonatophenyl)porphyrin, trisodium salt (**3**). The results showed compound **5** containing porphyrin moiety and **3** could interact with HSA. The quenching constant (K_{sv}) was 4.739×10^5 M^{-1} for **3**, and 2.846×10^5 M^{-1} for **5**; the apparent affinity binding constant (K_A) was 8.562×10^3 M^{-1} for **3**, and 4.978×10^4 M^{-1} for **5**.

KEYWORDS: dextran, nanoparticles, human serum albumin, interaction.

INTRODUCTION

Porphyrin compounds tend to accumulate in neoplastic tissue to higher concentrations than in surrounding normal tissue, and they might be photo-triggered to produce singlet-state oxygen and destroy the cancer cells when irradiated by light. Therefore, they have recently attracted significant attention in cancer diagnosis and treatment using photodynamic therapy (PDT) [1, 2]. As a potential valuable anti-tumor and antibiotic drug, porphyrin derivatives depend strongly on their physicochemical properties to enhance biological effects [3], and it is a challenge to formulate the porphyrin into chemically stable, effective, and safe dosage forms [4, 5].

Since it is now accepted that magnetic fields are not especially contraindicated for humans, except for patients whose body contains magnetizable material (medical devices with batteries or computer chips, vascular or intracranial metallic material), the use of magnetic micro- and nanoparticles has attracted increasing attention in the areas of biomedicine and biology, with a view to reducing the systemic distribution of cytotoxic compounds and enhancing uptake at the target site with effective treatment at lower dose [6–8]. The coating of polymer onto magnetic nanoparticles was applied to reduce aggregation and enhance the biocompatibility of the nanoparticles *in vivo* [9, 10]. Dextran is one of the candidates. Dextran is a water-soluble polysaccharide and its clinical use over the past 50 years has provided impressive safety and quality [11]. Recently, it has been investigated as a potential macromolecular carrier for delivery of drugs and proteins, primarily to increase the longevity of therapeutic agents [12].

Human serum albumin (HSA) is the major soluble protein constituent in the human circulatory system [13, 14], and plays an important role in metabolism, the transmission and distribution of fatty acids, amino acids, drugs and metal ions, and other functions. Therefore, it is important to study the interaction between drugs and HSA [15]. In the present work, we designed and synthesized the porphyrin-dextran Fe_3O_4 nanoparticles for the first time (Scheme 1), and investigated the interaction between **5** and HSA.

*Correspondence to: Kun Yan, email: kun_yan18@hotmail.com, tel: +86 27-87219084, fax: +86 27-68754067 and Zao-ying Li, email: zyliwuc@whu.edu.cn, tel: +86 27-87219084, fax: +86 27-68754067

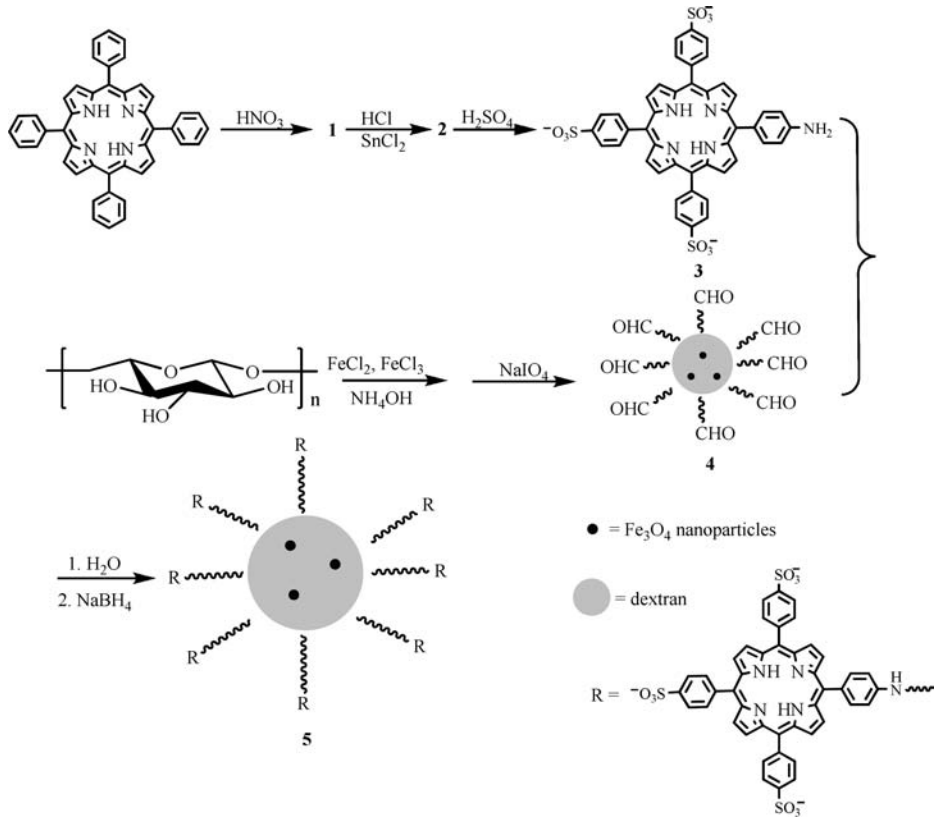

Scheme 1. Synthetic route of compound **5**

RESULTS AND DISCUSSION

With the addition of aqueous ammonia into the mixture solution of $FeCl_2$ and $FeCl_3$ in the presence of dextran, Fe_3O_4 nanoparticles coated with dextran were synthesized. Then the dextran-coated Fe_3O_4 was oxidized by $NaIO_4$ to produce the aldehyde (**4**). The size of **4** was smallest when the ratio of $FeCl_3$ to $FeCl_2$ was close to 2:1. In addition, the concentration of dextran, aqueous ammonia, as well as the stirring speed will all affect the size of **4** [16]. From porphyrin **3** and **4**, compound **5** was prepared by two consecutive steps: **3** was conjugated with **4** *via* Schiff base, then the corresponding C=N bond was reduced by $NaBH_4$. In order to describe the characteristic absorption band in FT-IR, we prepared the pure oxidized dextran specially. Figure 1 lines (a) and (b) shows the FT-IR spectra of oxidized dextran and **4**, respectively. Both exhibited an obvious peak at 1637 cm^{-1} in Fig. 1a,b due to the stretch vibration of -HC=O, but only in Fig. 1b could the peak at 646 cm^{-1} be observed, corresponding to the characteristics of Fe_3O_4 peak [17].

Porphyrin **3** shows max absorbed (Soret band) at 423 nm in UV-vis spectra [18], while the dextran shows no absorbance near the Soret band [19]. Therefore, the concentration of porphyrin moiety of **5** in solution was calculated with corresponding value at Soret band in UV-vis from the standard working curve of pure compound **3**. The porphyrin moiety in **5** was 35% of the entire molecular weight. The concentration of Fe in **5** was determined

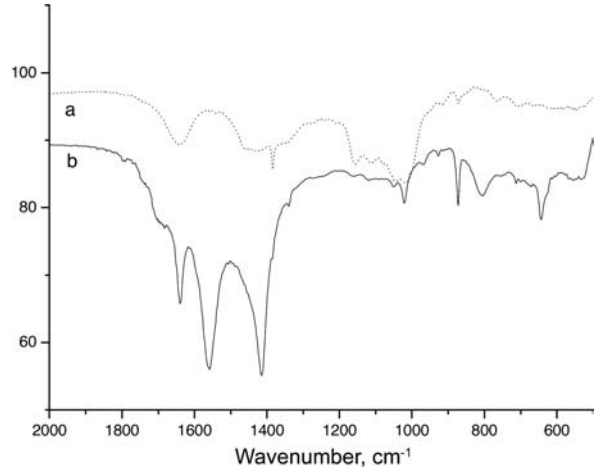

Fig. 1. The FT-IR spectra of (a) oxidized dextran and (b) compound **4**

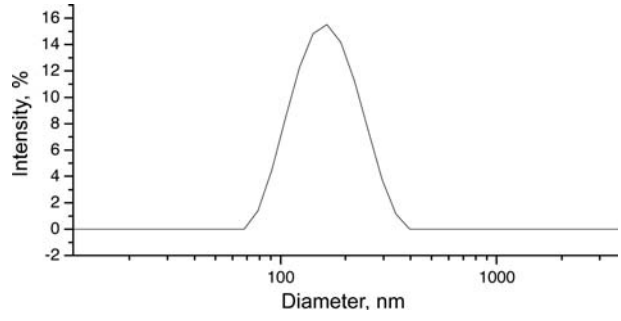

Fig. 2. Diameter distribution of compound **5** by DLS method

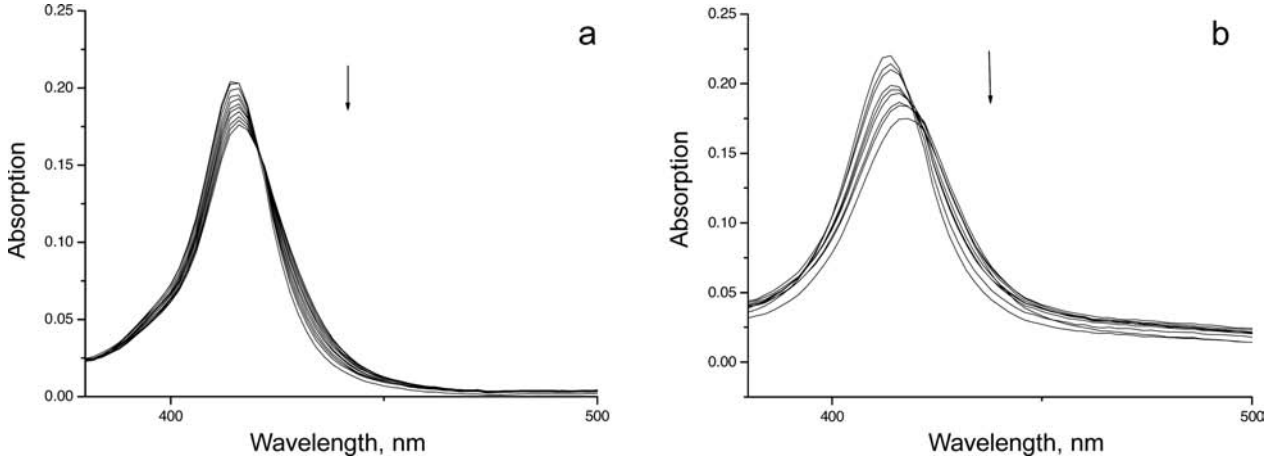

Fig. 3. The changes of UV-vis absorbance spectra of (a) **3** or (b) **5** with increasing concentration of HSA in PBS (pH = 7.4)

Table 1. Compared date of the interaction of **3** and **5** with HSA

Compound	UV-vis on the Soret band		Fluorescence emission
	Hypochromicity, %	Red shift, nm	Decrease of intensity, %
3	12.26	2	35.94
5	20.46	3	33.75

by ICP-AES to be 4.87 mg per gram. The diameter of **5** measured by DLS was about 204.9 nm (in Fig. 2).

The UV-vis absorbance changes to the porphyrin Soret band when HSA was titrated into compound **3** or **5** are shown in Fig. 3. As can be seen, the Soret band of both **3** and **5** red-shifted and showed hypochromism in different degrees [20, 21]. This indicates both compounds **3** and **5** are able to bind HSA. As summarized in Table 1, the Soret band of **5** exhibited 20.46% hypochromism when excess HSA was added. Only 12.26% hypochromism was observed for **3** under the same conditions, probably because the biocompatible dextran moiety made the binding between **5** and HSA easier and more efficient.

Fluorescence emission spectra for HSA with an increased concentration of compound **3** or **5** were recorded. With the titration of **3** or **5**, intensity of fluorescence emission of HSA presented a remarkable decrease as shown in Fig. 4a,b, respectively; the values are summarized in Table 1.

The quenching of HSA could be caused by either static quenching or dynamic quenching. The former could change the configuration and the bioactivities of HSA, while the latter was only a process of energy and electron transfer. Since the quenching accords with Stern-Volmer equation [22]:

$$F_0/F = 1 + K_{sv}(C) = 1 + K_q t_0(C) \quad (1)$$

($t_0 = 10^{-8}$ s, F, (C) were for the quenching intensity and concentration of **3** and **5**, respectively).

Figure 5a,b shows the average quenching constants of HSA in presence of **3** and **5**; the quenching constant (K_{sv}) and quenching velocity (K_q) are listed in Table 2.

From the value of K_q, it could be confirmed that static quenching happened between the HSA and **3** and **5**, for the maximum value of dynamic quenching velocity (K_q) was only 2.0×10^5 L.s.mol^{-1}, which was way smaller [23].

Based on the static quenching theory [24, 25], we obtained the apparent affinity binding constant (K_A) and

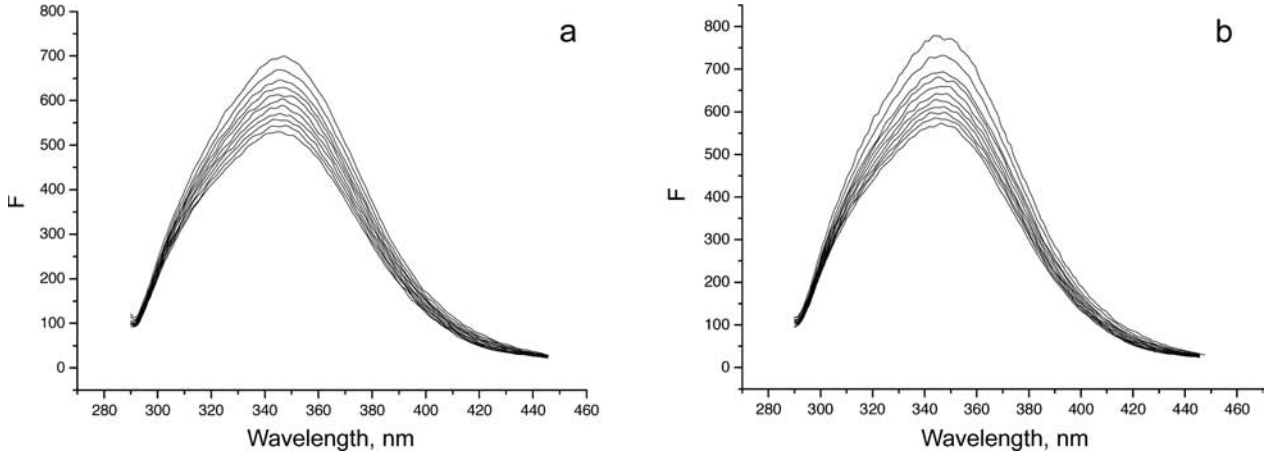

Fig. 4. Fluorescence emission spectra of HSA (2 μM) in PBS (pH = 7.4) with increasing concentration of (a) **3** or (b) **5** from 0 to 2 μM

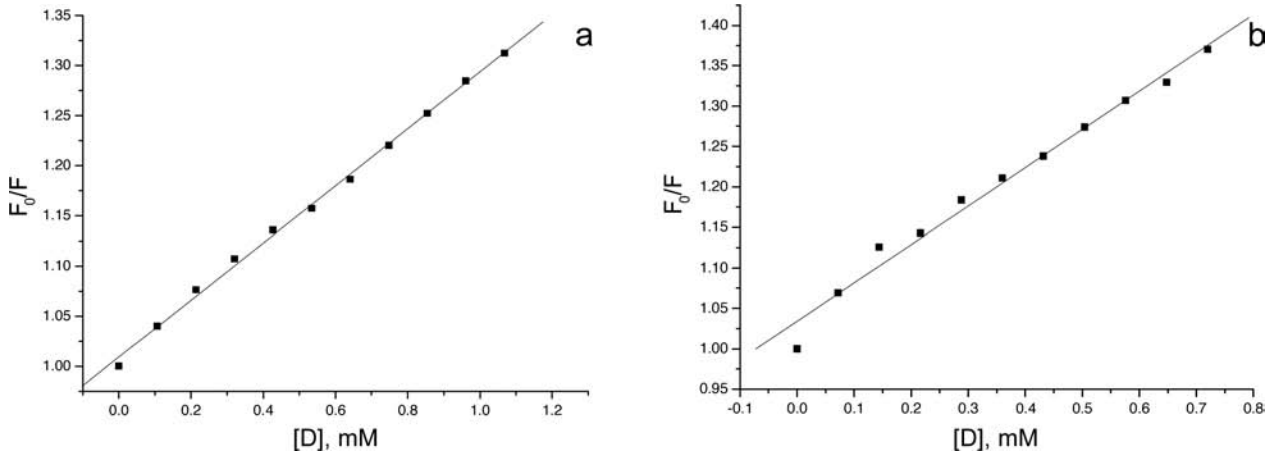

Fig. 5. The average quenching constants of HSA in presence of (a) **3** and (b) **5**

Table 2. The Stern-Volmer constants of fluorescence quenching of porphyrin-HSA

Compound	Stern-Volmer equation	K_{sv}, L.mol	K_q, L.s.mol^{-1}
3	$F_0/F = 1.009 + 2.846 \times 10^5$ C	2.846×10^5	2.846×10^{13}
5	$F_0/F = 1.034 + 4.739 \times 10^5$ C	4.739×10^5	4.739×10^{13}

Table 3. The apparent affinity binding constant (K_A) and the value of binding point (n) of porphyrin-HSA

Compound	Equation	K_A, M^{-1}	n
3	$\lg((F_0\text{-}F)/F) = 4.697 + 0.874 \lg((D))$	4.978×10^4	0.874
5	$\lg((F_0\text{-}F)/F) = 3.932 + 0.714 \lg((D))$	8.562×10^3	0.714

average binding point (n) of compounds **3** and **5** according to Equation 2. The data is tabulated in Table 3 and shown graphically in Fig. 6a,b.

$$lg((F_0 - F)/F) = K_A + nlg(C) \quad (2)$$

HSA has multiple binding sites for drug molecules. The primary binding sites of HSA are Site I and Site II. Site I involves the lone tryptophan residue of the protein (Trp-214), and fluorescence quenching is performed based on the intrinsic fluorescence of tryptophan residue. Site II contains a hydrophobic, branched, T-shaped cavity. According to published literature, if there were no binding sites other than Site I, the K_A would be smaller than K_{sv} [26]. As shown in Tables 2 and 3, the value of binding point (n) of both **3** and **5** was almost the same and the K_A was smaller than K_{sv}, which indicated that probably no other binding sites existed except for the one binding site near tryptophan [26]. In other words, it is probably the porphyrin moiety of **5** that was the only moiety located at the binding site in HSA. However, while the K_{sv} of **5** (4.739×10^5 M^{-1}) was bigger than that of **3** (2.846×10^5 M^{-1}), the K_A of **5** (8.562×10^3 M^{-1}) was smaller than that of **3** (4.978×10^4 M^{-1}). The K_{sv} is in response to the degree of fluorescence quenching. With the existence of dextran moiety in **5**, the porphyrin moiety should come into collision with HSA more easily and as a result quenched HSA more efficiently, and the deduction could explain the appearance in UV-vis absorbance spectra. The K_A represented the intensity of drug binding with HSA. The interaction between HSA and the porphyrin was a course of π-π stacking [27], and the steric resistance could be a greater factor. The size of **5** was much bigger than **3**, therefore the K_A value of **5** was smaller.

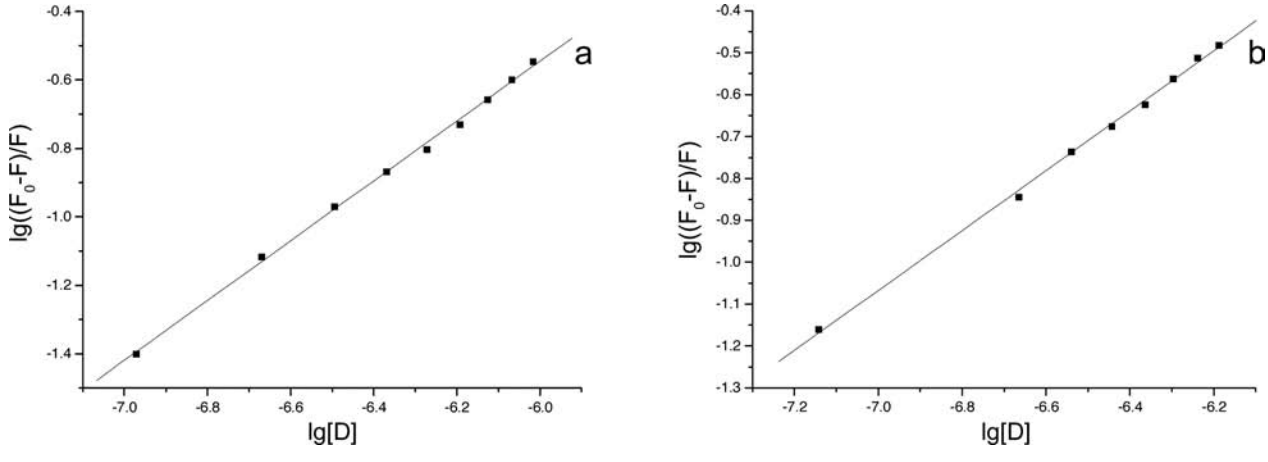

Fig. 6. The apparent affinity binding constant and binding point of porphyrin ((a) **3** or (b) **5**)-HSA

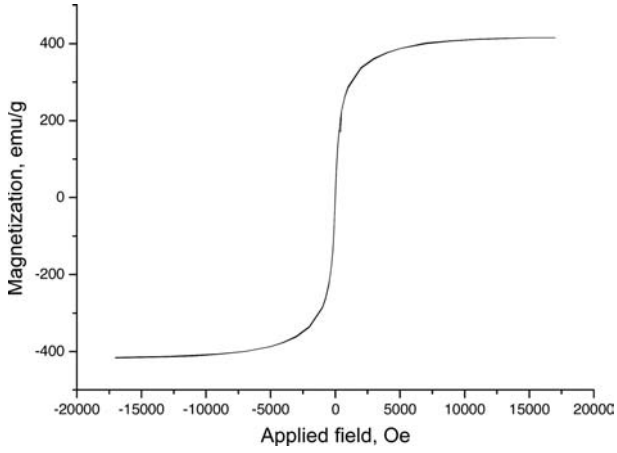

Fig. 7. Magnetization loop of compound **5**

Magnetization reflects the magnetic response capability. The greater the susceptibility of the samples, the higher the corresponding magnetic capacity. Figure 7 shows the magnetization loop of **5** measured at room temperature. As shown in Fig. 7, although with the intensification of the magnetic field, the value of magnetization increased, the relationship is nonlinear. When the magnetic field increased to a certain value, magnetization was unchanged, and at this moment magnetic saturation was reached. The saturation magnetization (Ms) of fine Fe_3O_4 particles was 415 emu.g^{-1}. The magnetization loop is a single curve over the starting point, and that means when the magnetic field was 0, there was no residual magnetism. In other words, Fig. 7 indicated that the Fe_3O_4 particles were superparamagnetic.

EXPERIMENTAL

General

All reagents and solvents were purchased from commercial sources and used without further purification. Chromatographic separations were performed using silica gel G (200–300 mesh). All UV-visible spectra were obtained on a Shimadzu 1601 spectrophotometer. Fluorescence spectra were recorded on PerkinElmer LS-55 fluorospectrophotometer. Proton NMR spectra were measured using a Varian Mercury VX 300 spectrometer.

In all measurements of interaction between compound **3** or **5** and HSA, individual components were dissolved respectively in phosphate buffer (PBS) with pre-adjusted pH, then pH was adjusted again in each solution before mixing, and the final pH value was verified thereafter. Buffer solution was made with bidistilled water.

Synthesis of compounds 1–5

Preparation of 5-(4-nitrophenyl)-10,15,20-triphenyl porphyrin (1). The synthesis of **1** was modified from literature methods [28]. Tetraphenylporphyrin (500 mg, 0.81 mmol) was dissolved in chloroform (150 mL). The solution was stirred, red fuming nitric acid (6.8 g, 108 mmol) was added at 0 °C over 2 h, and the solution was stirred for another 1 h. The reaction mixture was next diluted with ice water (100 mL), neutralized with saturation sodium hydroxide, then extracted with chloroform. The organic phase was dried over magnesium sulfate. The resulting solution was concentrated under reduced pressure. The residue solution was chromatographed on silica gel with chloroform as eluent to afford violet crystals (250 mg, 46% yield). IR (KBr): ν, cm^{-1} 1597 (NO_2). ^{1}H NMR ($CDCl_3$): δ_H, ppm 8.87 (d, 2 H, J = 5.2 Hz, β-pyrrole), 8.86 (s, 6 H, β-pyrrole), 8.54 (d, 2 H, J = 8.9 Hz, nitrophenyl), 8.30 (d, 2 H, J = 8.9 Hz, nitrophenyl), 8.19–8.21 (m, 6 H, ortho phenyl), 7.98–8.01 (m, 9 H, meta/para phenyls), -2.84 (s, 2 H, pyrrole NH). UV-vis ($CHCl_3$): λ_{max}, nm 418, 516, 552, 595, 645.

Preparation of 5-(4-aminophenyl)-10,15,20-triphenyl porphyrin (2). The synthesis of **2** was modified from the literature methods [28]. To compound **1** (200 mg, 0.3 mmol) in hydrochloric acid (50 mL, 6 M), tin(II) chloride dihydrate (3.0 g, 13.3 mmol) was added under nitrogen. The mixture solution was stirred at 60 °C for 1 h. The reaction mixture was neutralized with saturation sodium hydroxide to pH = 8 and extracted with chloroform. The organic phase was washed with water, followed by drying over magnesium sulfate. The solvent was concentrated under reduced pressure and the residue solution was chromatographed on silica gel with chloroform as eluent to give violet crystals (132 mg, 70% yield). ^{1}H NMR ($CDCl_3$): δ_H, ppm 8.95 (d, 2 H, J = 5.2 Hz, β-pyrrole), 8.84 (s, 6 H, β-pyrrole), 8.24–8.26 (m, 6 H, ortho phenyl), 7.96 (d, 2 H, J = 8.2 Hz, 4-aminophenyl), 7.70–7.72 (m, 9 H, meta/para phenyls), 7.06 (d, 2 H, J = 8.2 Hz, 4-aminophenyl), 4.02 (s, 2 H, amino), -2.74 (s, 2 H, pyrrole NH).

Preparation of 5-(4-aminophenyl)-10,15,20-tris-(4-sulfonatophenyl)porphyrin, trisodium salt (3). The synthesis of **3** was modified from literature methods [28]. The solution of compound **2** (100 mg, 0.16 mmol) in 30 mL sulfuric acid was heated to 70 °C for 48 h. The dark green solution was stirred under nitrogen for 72 h at room temperature. The reaction mixture was poured into 200 mL ice water and neutralized with saturated sodium hydroxide to pH = 8. The solution was concentrated under reduced pressure and methanol was added. After filtration, the precipitate was washed several times with methanol. The filtrate was combined and the solvent was evaporated to dryness. The residue was taken up in methanol and precipitated by addition of ethyl ether, then filtered off and dried under vacuum to afford violet crystals (97 mg, 65% yield). ^{1}H NMR (DMSO-d_6): δ_H, ppm 8.95 (s, 2 H, J = 5.1 Hz, β-pyrrole), 8.94 (s, 6 H, β-pyrrole), 8.17 (d, 6 H, J = 8.1 Hz, 4-sulfonatophenyl), 8.03 (d, 6 H, J = 8.2 Hz, 4-sulfonatophenyl), 7.86 (d, 2 H, J = 8.3 Hz, 4-aminophenyl), 7.01 (d, 2 H, J = 8.2 Hz, 4-aminophenyl), 5.56 (s, 2 H, amino), -2.84 (s, 2 H, pyrrole NH).

Preparation of oxidized dextran-coated Fe_3O_4 nanoparticles (4) [29]. Dextran T-40 (795 mg, 0.02 mmol), ferric chloride hexahydrate (48 mg, 24.1 mmol) and ferrous chloride tetrahydrate (129.3 mg, 45.8 mmol) were dissolved in H_2O (10 mL). Aqueous ammonia (7.5%, v/v) was added slowly into the above stirred solution (pH = 10–11) at 60 °C for 30 min. The aggregates were removed from the suspension by 3 cycles of centrifugation at 3000 R/min for 10 min. The solution of sodium periodate (5 mL, 5 mM) was added into the concentrated filtrate (5 mL). The mixture was stirred at room temperature for 1 h. The mixture was dialyzed overnight in sodium borate buffer (20 mM, pH = 8.5) at 4 °C. The residue was separated by gel filtration chromatography on Sephacryl 300, eluting with mixture solution of sodium acetate (0.1 M) and NaCl (0.15 M) at pH 6.5. The filtrate was freezed-dried and yellowy powder was obtained (215 mg, 22% yield). IR (KBr): ν, cm^{-1} 1637 (C=O), 646 (Fe-O).

Preparation of porphyrin-dextran-coated Fe_3O_4 nanoparticles (5). To compound **4** (300 mg) in H_2O (15 mL), compound **3** (100 mg, 0.11 mmol) was added. The mixture solution was stirred under nitrogen at room temperature for 8 h, followed by addition of sodium borohydride solution (10 mL, 5 mM). The mixture solution was stirred under nitrogen for 40 min. The reaction solution was dialyzed overnight in sodium borate buffer (20 mM, pH = 8.5) at room temperature. The residue was separated by gel filtration chromatography on Sephacryl 300, eluting with mixture solution of sodium acetate (0.1 M) and NaCl (0.15 M) at pH 6.5. The final residue was freezed-dried to afford violet powder (100 mg, 25% yield). IR (KBr): ν, cm^{-1} 3312 (pyrrole N-H), 1663 (C=O). UV-vis (H_2O): λ_{max}, nm 423 (Soret band), 520, 560, 596, 645 nm.

Measurement of iron concentration by ICP-AES

For the ICP-AES spectroscopy, the liquid sample was analyzed without pre-treatment. Fe concentration was calculated from the corresponding peak at 259.94 nm.

Measurement of the diameter of 5 with DLS

Compound **5** in PBS (particle density was 3.0 $g.cm^{-3}$) was used in the dynamic laser scattering (DLS) measurement. To avoid dust, the solution was filtered before performing the measurements.

UV-vis spectroscopy-titration

Titration of compounds **3** and **5** with HSA was performed at 25 °C in PBS (pH = 7.4). Determination of the HSA concentration was based upon the reported ε_{280} value of 35700 $M^{-1}.cm^{-1}$ by UV-vis absorbance spectra [30]. The concentration of porphyrin moiety of **5** was calculated from UV-vis absorbance spectra standard working curve of **3**. The starting volume of drug (compound **3** or **5**) solution was 3000 μL, and the total amount of HSA solution added was less than 100 μL. All results were averaged over at least five independent experiments.

HSA fluorescence quenching by 3 and 5

Compounds **3** and **5** were titrated into HSA at room temperature using excitation at 280 nm and emission at 340 nm. The excitation and emission slits were set at 15 and 20 nm, respectively. The concentration of porphyrin moiety of compound **5** was calculated from UV-vis absorbance spectra standard working curve of compound **3**. All results were averaged over at least five independent experiments.

Magnetic property measured

Magnetization loop was measured by a vibrating sample magnetometer (VSM) (Model 4AF-VSM, ADE Corporation, USA) at room temperature.

CONCLUSION

Novel porphyrin-dextran coated Fe_3O_4 nanoparticles (**5**) were designed and synthesized which could interact with HSA effectively due to the introduction of biocompatible dextran moiety. Compound **5** containing magnetic nanopartices moiety was superparamagnetic. The *in vivo* cellular uptake properties of **5** in the magnetic field are currently under investigation.

Acknowledgements

The present research has been financed by the National Natural Science Foundation of China (Grant CN 20672082).

REFERENCES

1. Dougherty TJ, Gomer CJ, Henderson BW, Jori G, Kessel D, Korbelik M, Moan J and Peng Q. *J. Natl Cancer Inst.* 1998; **90**: 889–905.
2. Ali H and van Lier JE. *Chem. Rev.* 1999; **99**: 2379–2450.
3. Yushmanov VE, Tominaga TT, Borissevitch IE, Imasato H and Tabak M. *Magn. Reson. Imaging* 1996; **14**: 255–261.
4. Kongshaug M, Moan J and Brown SB. *Brit. J. Cancer* 1989; **59**: 184–188.
5. Korbelik M and Hung J. *Photochem. Photobiol.* 1991; **53**: 501–510.
6. Wang L, Yang ZM, Gao JH, Xu KM, Gu HW, Zhang B, Zhang XX and Xu B. *J. Am. Chem. Soc.* 2006; **128**: 13358–13359.
7. Lim YT, Lee KY, Lee K and Chung BH. *Biochem. Biophys. Res. Commun.* 2006; **344**: 926–930.
8. Lewin M, Carlesso N, Tung CH, Tang XW, Cory D, Scadden DT and Weissleder R. *Nature Biotechnol.* 2000; **18**: 410–414.

9. Lind K, Kresse M, Debus NP and Muller RH. *J. Drug Target* 2002; **10**: 221–230.
10. Bellin MF, Beigelman C and Precetti-Morel S. *Eur. J. Radiol*. 2000; **34**: 257–264.
11. Kumashiro Y, Huh KM, Ooya T and Yui N. *Biomacromolecules* 2001; **2**: 874–879.
12. Mehvar R. *J. Control. Release* 2000; **69**: 1–25.
13. Kragh-Hansen U. *Pharmacol. Rev.* 1981; **33**: 17–53.
14. Carter DC and Ho JX. *Adv. Protein Chem.* 1994; **45**: 153–203.
15. Eckenhoff RG, Petersen CE, Ha CE and Bhagavan NV. *J. Biol. Chem.* 2000; **275**: 30439–30444.
16. Hong YR, Feng B, Chen LL, Liu GH, Li HZ, Zeng Y and Wei DG. *Biochem. Eng. J.* 2008; **42**: 290–300.
17. Kim GC, Li YY, Chu YF, Cheng SX, Zhang XZ and Zhuo RX. *J. Biomater. Sci.-Polym. Ed.* 2008; **19**: 1249–1259.
18. Meng GZ, James BR, Skov KA and Korbelik M. *Can. J. Chem.* 1994; **72**: 2447–2457.
19. Ramanujam PS. *Opt. Mater.* 2005; **27**: 1175–1177.
20. Yin YB, Wang YN and Ma JB. *Spectrochim. Acta. A* 2006; **64**: 1032–1038.
21. Andrade SM and Costa SMB. *Chem.-Eur. J.* 2006; **12**: 1046–1057.
22. Eftink MR and Ghiron CA. *Anal. Biochem.* 1981; **114**: 199–227.
23. Liu XF, Xia YM, Fang Y, Liu LL and Zou L. *Chem. J. Chin. Univ. (Chinese)* 2004; **25**: 2099–2103.
24. Wilson DF. *Adv. Exp. Med. Biol.* 1992; **317**: 195–201.
25. Chakrabarty A, Mallick A, Haldar B, Das P and Chattopadhyay N. *Biomacromolecules* 2007; **8**: 920–927.
26. Zhou B, Zhang Z, Zhang Y, Li R, Xiao Q, Liu Y and Li ZY. *J. Pharm. Sci.* 2009; **98**: 105–113.
27. Moan J, Rimington C and Western A. *Clin. Chim. Acta* 1985; **145**: 227–236.
28. Meng GZ, James BR, Skov KA and Korbelik M. *Can. J. Chem.* 1994; **72**: 2447–2457.
29. Hong X, Guo W, Yuan H, Li J, Liu YM, Ma L, Bai YB and Li TJ. *J. Magn. Magn. Mater.* 2004; **269**: 95–100.
30. Andrade SM and Costa SMB. *Biophys. J.* 2002; **82**: 1607–1619.